



Article

Localized Expression of Olfactory Receptor Genes in the Olfactory Organ of Common Minke Whales

Ayumi Hirose ^{1,2,*}, Gen Nakamura ², Masato Nikaido ¹, Yoshihiro Fujise ³, Hidehiro Kato ^{2,3}
and Takushi Kishida ^{4,5}

¹ School of Life Science and Technology, Tokyo Institute of Technology, Tokyo 152-8550, Japan; mnikaido@bio.titech.ac.jp

² Department of Ocean Sciences, Tokyo University of Marine Science and Technology, Tokyo 108-8477, Japan

³ The Institute of Cetacean Research, Tokyo 104-0055, Japan

⁴ Museum of Natural and Environmental History, Shizuoka 422-8017, Japan; kishida.takushi@nihon-u.ac.jp

⁵ College of Bioresource Sciences, Nihon University, Fujisawa 252-0880, Japan

* Correspondence: hirose.a.ad@m.titech.ac.jp

Abstract: Baleen whales (Mysticeti) possess the necessary anatomical structures and genetic elements for olfaction. Nevertheless, the *olfactory receptor* gene (*OR*) repertoire has undergone substantial degeneration in the cetacean lineage following the divergence of the Artiodactyla and Cetacea. The functionality of highly degenerated mysticete *ORs* within their olfactory epithelium remains unknown. In this study, we extracted total RNA from the nasal mucosae of common minke whales (*Balaenoptera acutorostrata*) to investigate *ORs'* localized expression. All three sections of the mucosae examined in the nasal chamber displayed comparable histological structure. However, the posterior portion of the frontoturbinal region exhibited notably high *OR* expression. Neither the olfactory bulb nor the external skin exhibited the expression of these genes. Although this species possesses four intact non-class-2 *ORs*, all the *ORs* expressed in the nasal mucosae belong to class-2, implying the loss of aversion to specific odorants. These anatomical and genomic analyses suggest that *ORs* are still responsible for olfaction within the nasal region of baleen whales, enabling them to detect desirable scents such as prey and potential mating partners.

Keywords: epithelium; histology; Mysticeti; nasal complex; olfaction; RNA-seq; secondary-aquatic



Citation: Hirose, A.; Nakamura, G.; Nikaido, M.; Fujise, Y.; Kato, H.; Kishida, T. Localized Expression of Olfactory Receptor Genes in the Olfactory Organ of Common Minke Whales. *Int. J. Mol. Sci.* **2024**, *25*, 3855. <https://doi.org/10.3390/ijms25073855>

Academic Editor: Brad Freking

Received: 21 February 2024

Revised: 13 March 2024

Accepted: 20 March 2024

Published: 29 March 2024



Copyright: © 2024 by the authors. Licensee MDPI, Basel, Switzerland. This article is an open access article distributed under the terms and conditions of the Creative Commons Attribution (CC BY) license (<https://creativecommons.org/licenses/by/4.0/>).

1. Introduction

Olfaction, the sense of smell, is one of the sensory modalities encompassing biologically important behaviors such as foraging, predator avoidance, mother–calf relationships, mating, and territorial display [1–3]. The sense of smell arises when olfactory receptor proteins within the nasal cavity capture volatile chemical substances. These proteins are localized on the membranes of olfactory cells. Stimulation is subsequently transmitted from the receptor protein through the cribriform plate into the main olfactory bulb by olfactory nerves, extending from the base of olfactory cells. Olfactory receptor genes (*ORs*) are responsible for encoding these olfactory receptor proteins [4]. *ORs* comprise the largest gene family in mammals and are broadly classified into two categories—class-2 and non-class-2—based on their nucleotide sequences [5,6]. In certain studies, non-class-2 *ORs* are referred to as ‘class-1 *ORs*’. Each *OR* encodes a specific olfactory receptor protein that interacts with particular ligands, enabling the discrimination between different odors [7,8].

The observed variation in mammalian olfaction is recognized as a result of anatomical and genomic factors, as described by the aforementioned mechanism. Anatomical features, such as the cribriform plate dimensions [9], generally align with olfactory abilities, exhibiting interspecies variations. Furthermore, an augmented number of *OR* copies within a species denotes an elevated discriminatory capacity and enhanced olfactory significance [10,11]. Primate olfactory organs are comparatively smaller than other mammals,

indicating a reduced olfactory capacity within the human species (*Homo sapiens*) [12,13]. Consistently, humans possess approximately 400 copies of ORs [14], which is remarkably fewer than the approximate 1000 copies found in mice (*Mus musculus*) or rats (*Rattus norvegicus*) [15]. Both morphological investigations and genomic studies support the diminished importance of olfaction in humans.

The main olfactory organ in mammals is positioned within the respiratory passage, enabling the detection of odors with each inhalation. At this juncture, a query arises: can this sensory system suffice for fully aquatic mammals? Cetaceans, having transitioned into an aquatic environment over 50 million years ago [16–19], encompass two distinct monophyletic lineages known as baleen whales (Mysticeti) and toothed whales (Odontoceti) [20]. They breathe air solely when they ascend to the water's surface. Although the frequency of breaths may vary based on activity levels, consistent breathing patterns have been observed across numerous species. For instance, small-toothed whales generally breathe every 1–2 min, killer whales (*Orcinus orca*) breathe no more than every 8 min, and deep-diving species such as sperm whales (*Physeter macrocephalus*) and beaked whales (Ziphiidae) can remain submerged for approximately 1 h [21]. In the case of baleen whales, blue whales (*Balaenoptera musculus*) typically exhibit breathing intervals of approximately 4 min [21]. Humpback whales (*Megaptera novaeangliae*) demonstrate an average interdive breathing interval of 6 min and 45 s during the breeding season. In some instances, particularly among singers (male whales which repeatedly emit patterned sequences of sounds), this interval can extend to approximately 13 min [22,23]. Consequently, cetaceans experience periods of interrupted respiration during dives, leading to the intermittent reception of sensory information through the olfactory modality.

Recently, baleen whales' olfactory capabilities have been investigated through morphological and genomic studies [24–30]. The skeletal components of the main olfactory organ, such as the cribriform plate and turbinals, have been observed in common minke whales (*Balaenoptera acutorostrata*) [24,25]. In this species, the nasal mucosa covering the cribriform plate demonstrates similarities to the olfactory mucosa found in terrestrial mammals, as it is lined with pseudostratified columnar epithelium and glandular organs like Bowman's gland within the lamina propria [26]. Gross and microscopic examinations have supported the presence of the main olfactory organ in bowhead whales (*Balaena mysticetus*) [27,28], and subsequent immunohistochemical staining has identified olfactory nerves in the nasal mucosa of this species [29]. Han et al. [30] conducted a search for ORs in seven baleen whale species using publicly available whole genomes, annotating between 54 and 95 intact OR copies. The number of ORs identified in baleen whales is lower than in other mammals and corresponds to the reduced anatomical complexity of their main olfactory organ.

Both morphological and genomic investigations postulate cetacean hyposmia. This diminished olfactory capability is discernible following the divergence of Artiodactyla and Cetacea [31]. However, baleen and toothed whales exhibit this reduction in distinct manners. While the aforementioned genomic studies suggest a relatively less efficient sense of smell in baleen whales than in terrestrial mammals, they possess a larger repertoire of ORs than toothed whales [30–33]. Analysis of the *olfactory marker protein* gene (*OMP*), which exhibits high expression in the olfactory epithelium and plays a crucial role in olfaction [34,35], indicates that the sense of smell in baleen whales is subjected to purifying selection pressures, whereas toothed whales experience more relaxed selective pressures [36,37]. Furthermore, baleen whales exhibit anatomical features essential for olfaction similar to those found in terrestrial mammals. By contrast, the nasal morphology of extant toothed whales has undergone significant modifications for biosonar signal generation, and it is widely accepted that olfactory structures are absent in this lineage [38–40]. Airborne odorants have been proposed to serve as a locating cue for krill, attracting baleen whales through olfactory modality rather than toothed whales [27,31]. Behavioral experiments targeting humpback whales, long-finned pilot whales (*Globicephala melas*), and bottlenose dolphins (*Tursiops truncatus*) have supported this hypothesis [41,42]. The sense of olfaction provides a captivating illustration of how cetaceans interact with their aquatic environment, primarily due to the accelerated evolutionary rate

observed in placental mammals' ORs [33]. The remarkable diversification of ORs highlights their vital role in shaping species diversity through olfactory perception.

While exploring ORs provides a powerful methodology for evaluating olfactory capabilities, it has certain limitations in comprehending the sense of smell [43]. It is important to note that not all ORs are exclusively expressed within the olfactory mucosa, which is intricately linked to olfactory reception [44]. The existence of ectopic ORs, expressed in various non-olfactory tissues, has been documented [45]. Notably, specific ORs in humans and mice exhibit expression in the testis and participate in sperm chemotaxis [46–49]. Furthermore, a gene known as *OR51E2*, classified as a non-class-2 OR is present in nearly all mammalian species, including both baleen and toothed whales [30], and has been identified in the prostate [50]. Hence, the mere presence of ORs does not unequivocally signify odor detection capabilities.

Prior investigations have established that baleen whales possess the essential anatomical structures and genetic elements for olfaction; however, these findings alone do not guarantee the existence of a sense of smell based on the same mechanism as observed in other mammals. Therefore, the objective of the present study was to determine whether intact ORs are exclusively expressed in the mucosa of the putative main olfactory organ in baleen whales or not. To address this objective, we used the common minke whale as our research subject and extracted total RNA from the nasal mucosa to examine localized OR expression.

2. Results

2.1. Gross Observation

Three distinct nasal turbinals were observed in the medial aspect of the nasal chamber in all the investigated animals (Figures 1 and 2, Table 1). These structures were identified as the lamina semicircularis, ethmoturbinals I and II. The configuration of these nasal turbinals closely resembles the 'ethmoturbinates/olfactory recess' described in common minke whales (Figures 6 and 7 in Godfrey et al. [24]), as well as bowhead whales (Figure 7 in Farnkopf et al. [29]).

Table 1. List of specimens.

Location	Year	ID	Sex	Body Length (m)	PMI [†] (h)	Description of Specimen	Side	Techniques Used	Sample ID
Kushiro, Hokkaido	2016	16NPCK-M009	M	7.01	4.5	Nasal mucosa	L	Histology	H-009
Kushiro, Hokkaido	2018	18NPCK-M001	M	5.50	6	Nasal mucosa (Ethmoturbinal II)	L	RNA-seq Histology	R-001 H-001
		18NPCK-M006	M	7.09	6	Nasal mucosa (Frontoturbinal)	L	RNA-seq	R-006
		18NPCK-M008	F	4.62	6	Olfactory bulb	R	RNA-seq	R-008
Abashiri, Hokkaido	2018	18NPCO-M046	F	7.30	5	Nasal mucosa (Anterior portion)	R	RNA-seq Histology	R-046 H-046
Kushiro, Hokkaido	2019	19SK214	M	6.96	8.5	External skin	-	RNA-seq	R-214
		19SK215	M	7.33	5.5	External skin	-	RNA-seq	R-215

[†] PMI means the post-mortem interval.

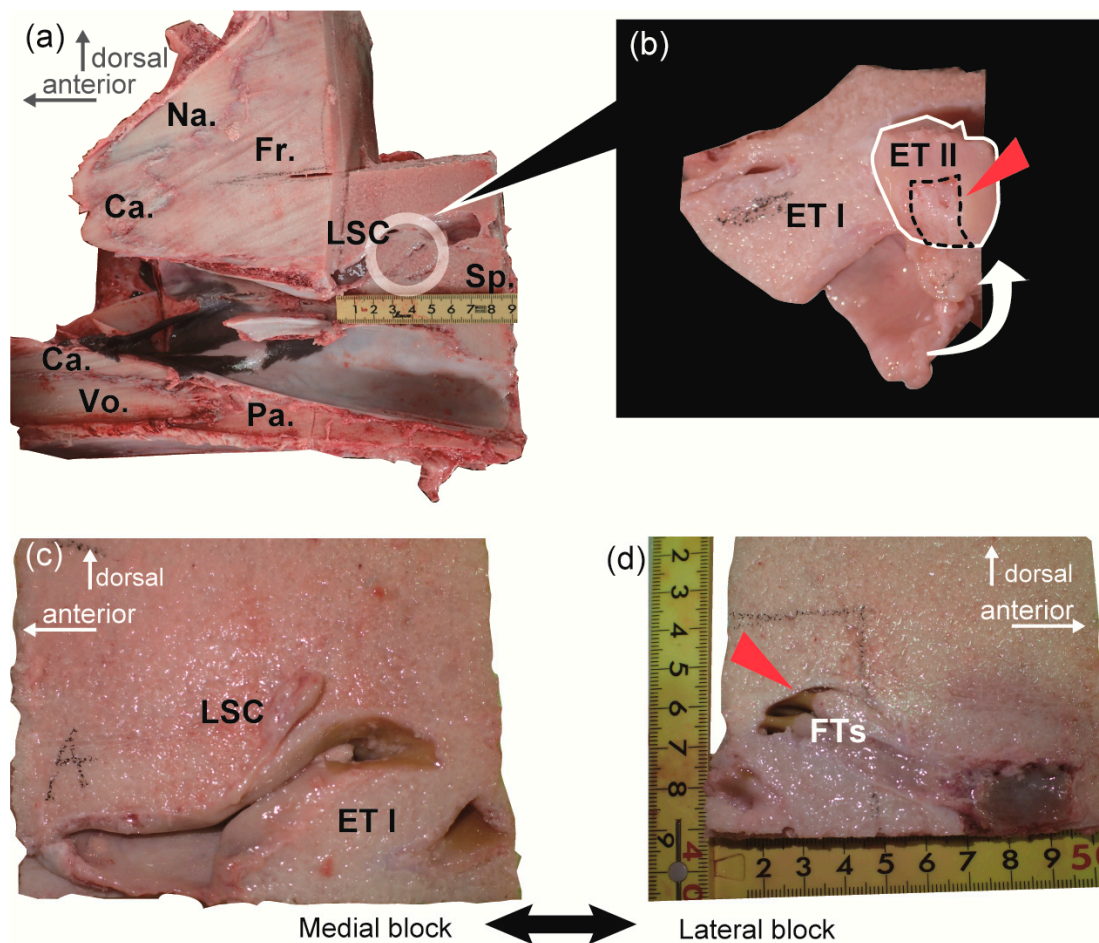


Figure 1. Portions where samples R-001, H-001, and R-006 were harvested. (a) A lateral view of a parasagittal section of the cranium from 18NPCK-M001 illustrates the localization of the nasal turbinals (marked by a white circle) within the left nasal chamber. (b) An enlarged view of the ethmoturbinals I and II positioned anteriorly to the cribriform plate. The highlighted region, delineated by a white line, represents the posterior end of the ethmoturbinal II. To expose its medial side, this segment was folded over (white arrow). The red arrowhead denotes the site of mucosal sample R-001 extraction (enclosed by a dashed line). Additionally, histological sample H-001 was obtained in proximity to this area. (c) A parasagittal section of the left nasal chamber from 18NPCK-M006. This section, depicted in a medial block, provides a lateral view. (d) The corresponding lateral side (in medial view) of the section shown in (c). This photograph displays two frontoturbinals. Mucosal sample R-006 was collected from the posterior-most region of the dorsal frontoturbinal (indicated by the red arrowhead). Abbr: Ca., cartilage; ET I and II, ethmoturbinal I and II, respectively; Fr., frontal bone; FT, frontoturbinal; LSC, lamina semicircularis; Na., nasal bone; Pa., palatine bone; Sp., presphenoid bone; Vo., vomer bone.

The cranial bony block from 16NPCK-M009 exhibited a complicated morphology of nasal turbinals situated laterally to the ethmoturbinals I and II (Figure 2). The ethmoturbinal I was positioned anteriorly to the olfactory bulb chamber and was accompanied ventrolaterally by the posterior part of ethmoturbinal I (Figure 2b, ET I p). Lateral to the ethmoturbinal I, the dorsal region of the nasal chamber was occupied by two slender frontoturbinals (Figure 2b, FT) that corresponded to the same area from which R-006 was obtained (Figure 1c,d). A relatively small turbinal structure, known as the interturbinal (Figure 2b, IT) was located lateral to the ethmoturbinal II.

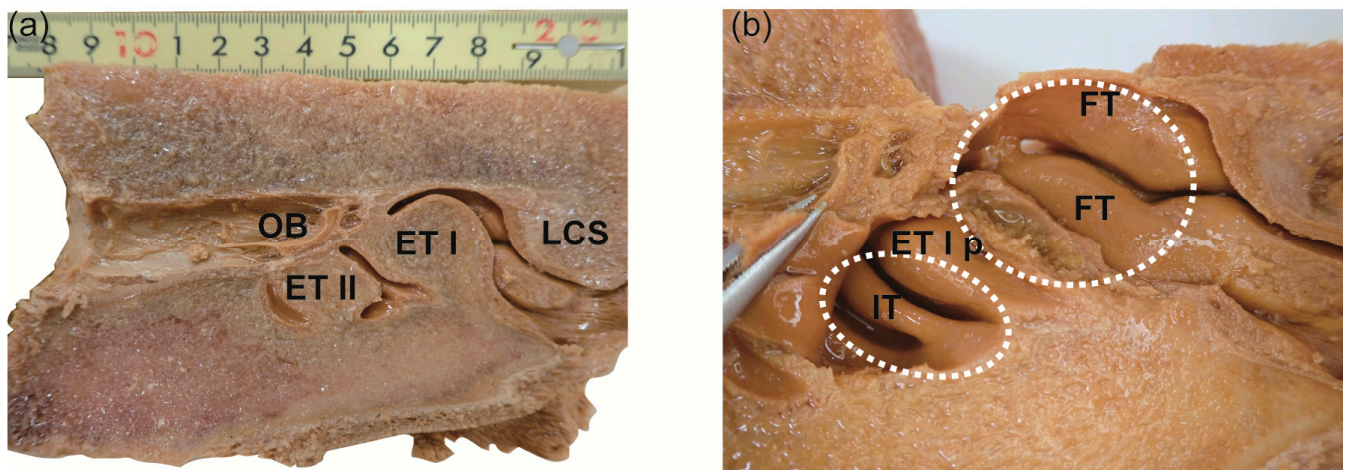


Figure 2. The parasagittal section of the left nasal chamber of 16NPCK-M009. (a) Medial view of the nasal chamber and the posteriorly adjoining olfactory bulb chamber. (b) A closer medial view of the nasal chamber following removal of ethmoturbinals I and II. The lateral region of the nasal chamber becomes visible. The regions previously occupied by the ethmoturbinals I and II are indicated by circles outlined with white dashed lines. The left and bottom sides correspond to the posterior and ventral directions, respectively. Abbr: ET I and II, ethmoturbinal I and II, respectively; ET I p, ethmoturbinal I posterior part; FT, frontoturbinal; IT, interturbinal; LSC, lamina semicircularis; OB, olfactory bulb.

2.2. Expression of the Olfactory Receptor Genes

Transcriptome sequencing using RNA-seq was performed on the nasal mucosae of the putative olfactory organ (R-001, R-006, R-046), the olfactory bulb (R-008), and the external skin (R-214 and R-215) of common minke whales. The FPKM values of β -actin were as follows: R-001, 983; R-006, 285; R-046, 549; R-008, 371; R-214, 161; R-215, 143 (Table 2), indicating successful RNA extraction from all the samples. In this study, 81 intact ORs, 12 pseudogenes, and 266 truncated genes were annotated (Supplementary file S1). The maximum expression level (as a percentage of FPKM for β -actin) of intact ORs in negative controls (the olfactory bulb, R-008, and external skin, R-214 and R-215) was 0.749 of R-008 (Figure 3). The average expression of intact ORs with non-zero expression across all samples was 1.014. This expression level was used as the criterion for expression in this study.

Table 2. FPKM and calculated expression percentage.

	R-001	R-006	R-046	R-008	R-214	R-215
β actin (FPKM)	983	285	549	371	161	143
<i>OMP</i>						
FPKM	9.510	21.101	0	0	0	0
Expression †	0.966	7.378	0	0	0	0
Average of expressing intact ORs						
FPKM	3.640	6.537	0.244	0.543	0.171	0.112
	± 4.946	± 8.735	± 0.372	± 0.876	± 0.098	± 0.054
Expression †	0.370	2.286	0.045	0.146	0.106	0.078
	± 0.503	± 3.054	± 0.068	± 0.236	± 0.061	± 0.038

† Expression (%) was calculated as follows: FPKM of a gene was divided by that of β actin, then multiplied by 100.

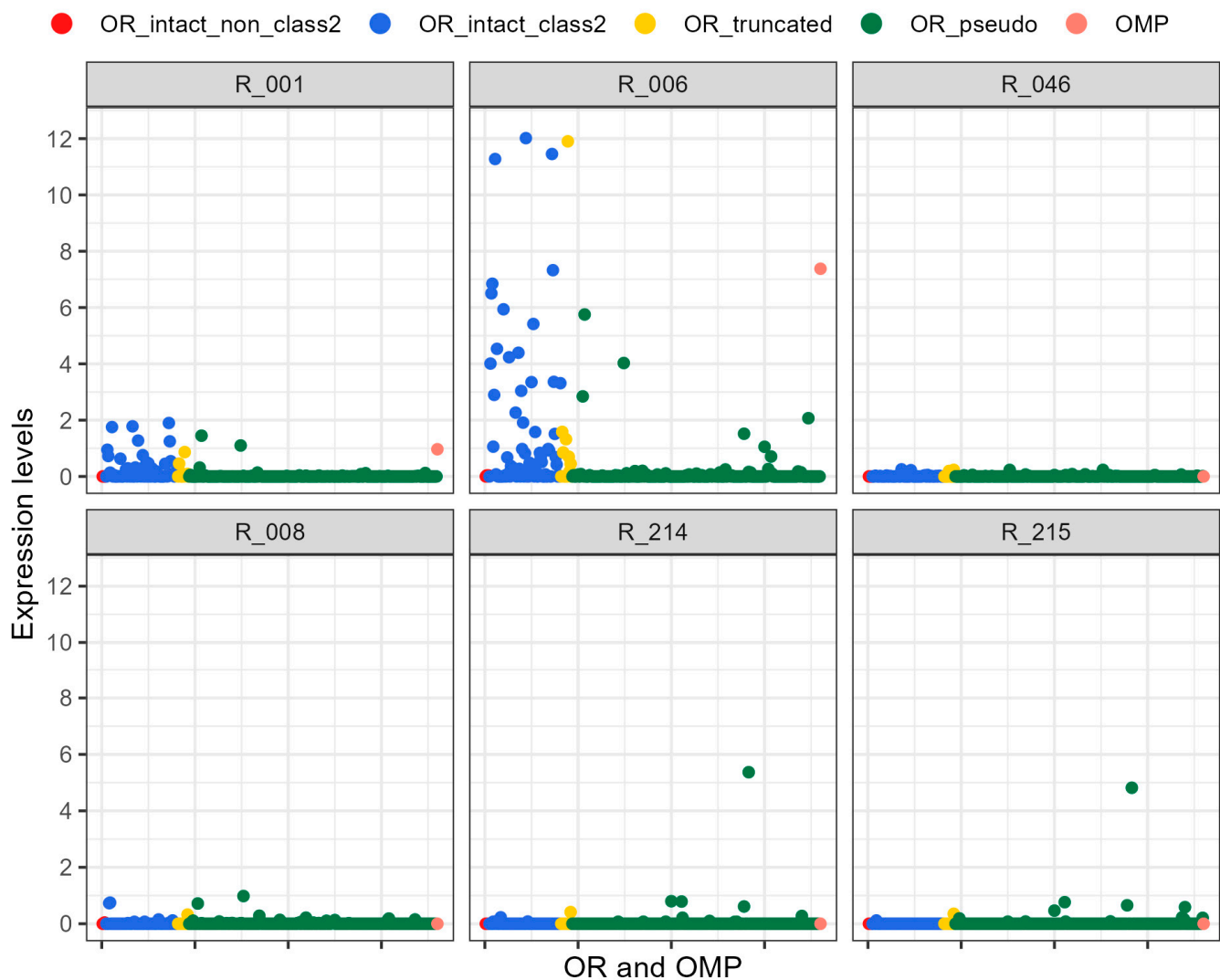


Figure 3. Expression of ORs and OMP. R-001, R-006, and R-046 correspond to the nasal mucosae of the ethmoturbinal II, frontoturbinal, and anterior nasal chambers, respectively. R-008 originated from the olfactory bulb, and both R-214 and R-215 were obtained from the external skin. The average expressions of intact ORs exhibiting non-zero expression were as follows: R-001, 0.370 ± 0.503 ; R-006, 2.286 ± 3.054 ; R-046, 0.045 ± 0.068 ; R-008, 0.146 ± 0.236 ; R-214, 0.106 ± 0.061 ; R-215, 0.078 ± 0.038 .

Among the nasal mucosa samples, R-006 from the frontoturbinal (Figure 1b) exhibited the expression of 22 intact ORs, while five of them were also expressed in R-001 from the ethmoturbinal II (Figure 1d). OMP, on the other hand was exclusively expressed in R-006, with an expression level greater than 1.014. By contrast, R-046, obtained from the anterior portion of the nasal chamber, did not demonstrate sufficient expression of ORs or OMP for our criterion of 1.014. Out of the 81 annotated intact ORs, all the genes expressed in the nasal mucosa samples belonged to class-2 ORs. Although four copies of intact non-class-2 ORs were annotated, none were expressed in the six investigated samples (expression levels were between 0 and 0.045). The expressed intact ORs did not form a cluster in the phylogenetic tree (Figure 4). Note, that some pseudogenes were highly expressed in the nasal mucosa, and one pseudogene was exclusively expressed in the external skin, as per our investigation.

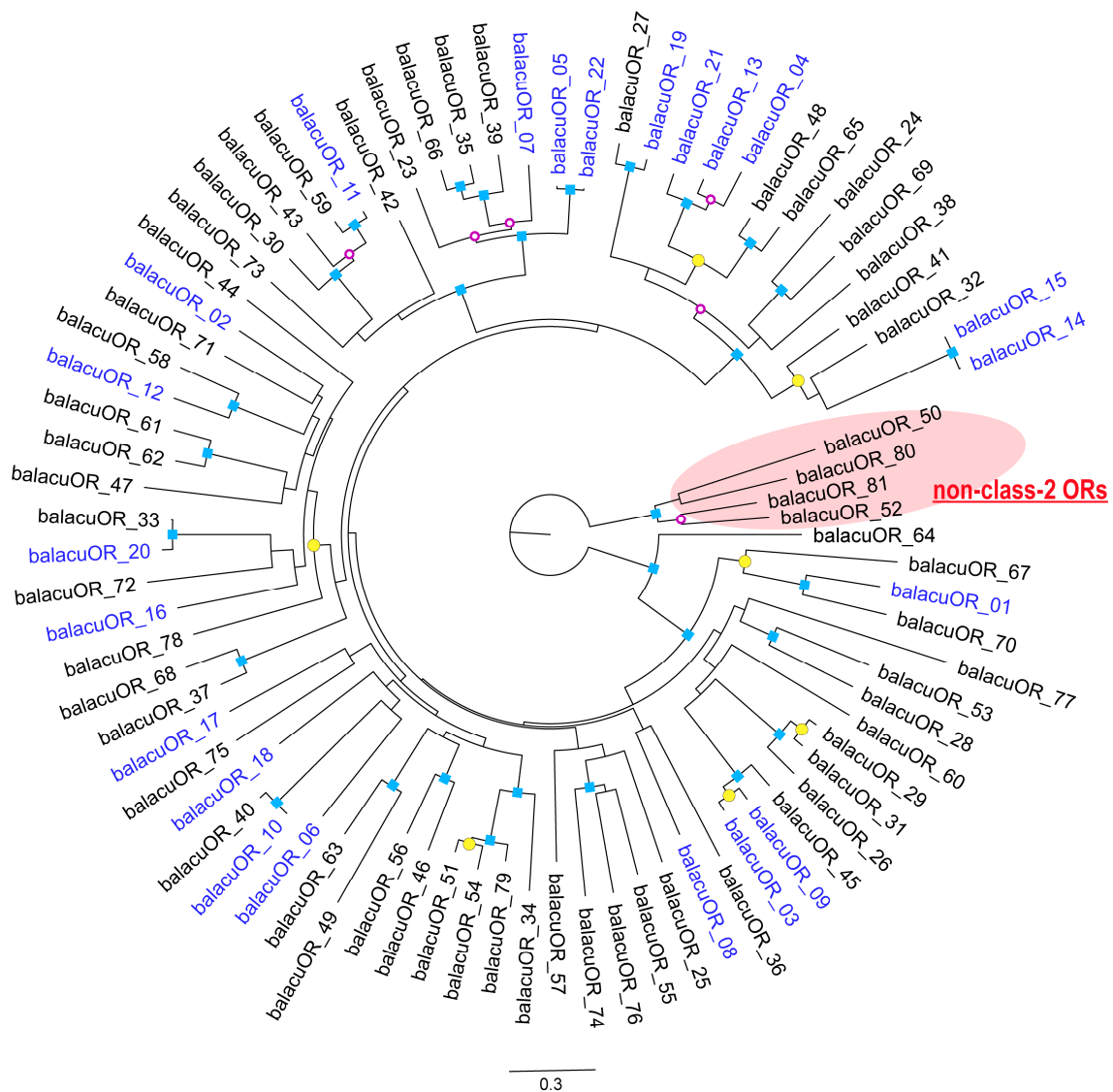


Figure 4. Phylogenetic tree constructed from intact ORs. Genes labeled in blue were determined to be expressed in R-006. The root of the tree was established based on non-class-2 ORs. Nodes displaying bootstrap values of 100, 86–99, and 71–83 are denoted by blue squares, yellow circles, and open circles outlined in purple, respectively. Nodes with bootstrap values below 70 are not marked.

2.3. Histological Staining

Histological examination of the nasal mucosae (H-001, H-009, and H-046) revealed that they were all covered with pseudostratified columnar epithelium and contained glands with orifices (Figure 5, Table 3). These glands appeared to be serous glands, and goblet cells were not observed. In all three mucosae, a nucleus-free zone was observed between the apical surface of the epithelium and the nuclei of supporting cells. This phenomenon was particularly evident in H-009, the sample harvested from the frontoturbinal. Additionally, peripheral nerves were distributed beneath the lamina propria in H-009 (Figure 5).

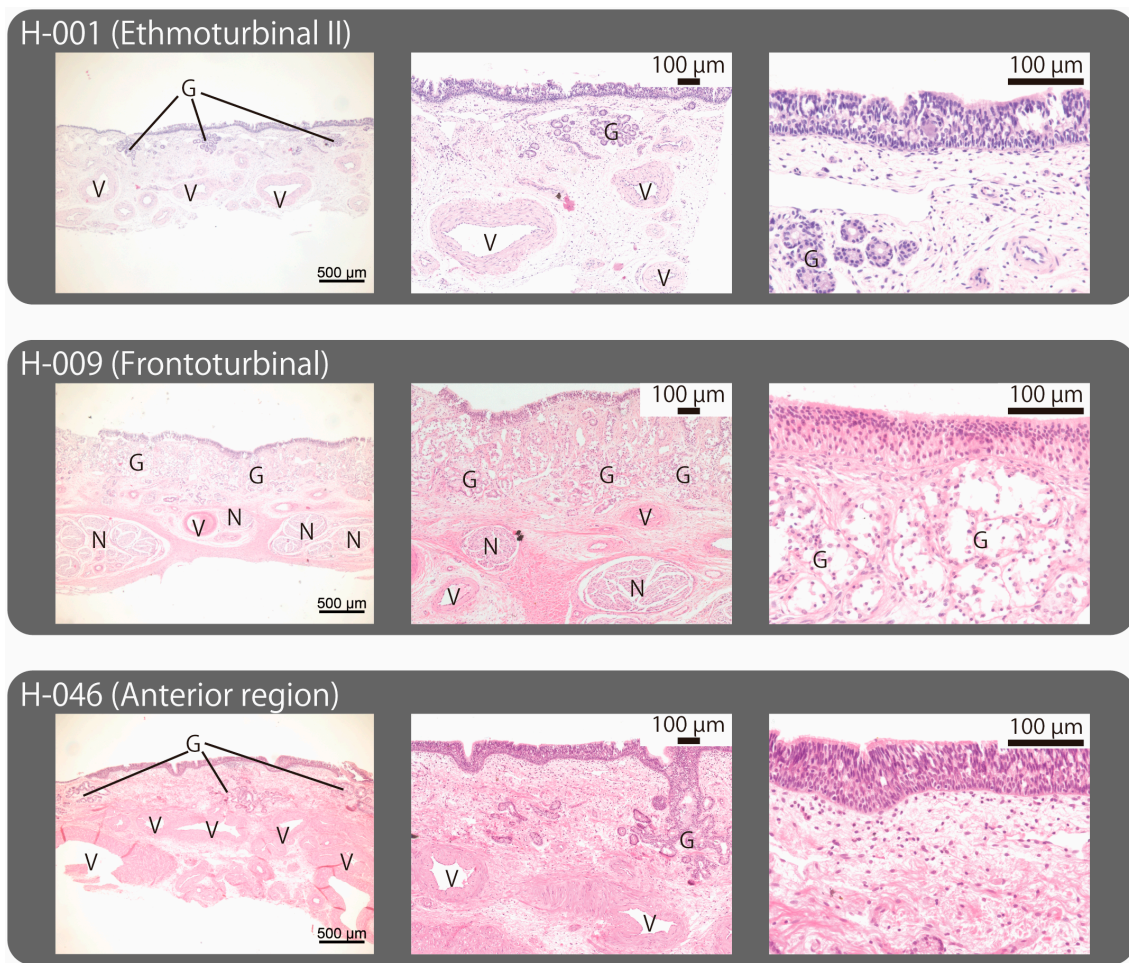


Figure 5. Microscopic views of mucosal samples. The scale bars in the photographs in the far-left, center, and far-right columns are 500 µm, 100 µm, and 100 µm, respectively. The nasal cavity is located at the top of each image. Abbr: G, glands; N, peripheral nerve; V, blood vessel.

Table 3. Results of RNA-seq and histological observation of mucosal samples.

Description of Specimen	Sample ID	OR Expression	OMP Expression	Pseudostratified Columnar Epithelium	Bowman's Glands	Absence of Goblet Cells	Nucleus Free Zone	Peripheral Nerve
Ethmoturbinal II	H-001 R-001	low	low	Y	Y	Y	Y	N
Frontoturbinal	H-009 R-006	Y	Y	Y	Y	Y	Y	Y
Anterior portion	H-046 R-046	N	N	Y	Y	Y	Y	N

3. Discussion

This study confirmed the specific expression of 22 *OR* copies in the posterior region of the nasal chamber in common minke whales. The *ORs* were predominantly expressed in the posterior portion of the nasal chamber, facing toward the olfactory bulb, with higher expression levels observed in the frontoturbinal region (R-006) and moderately in the ethmoturbinal II (R-001). Previous reports noted that these nasal turbinals are covered with the olfactory epithelium in typical mammals [51]. Furthermore, the *OMP* expression level was highest in sample R-006, indicating that the posterior portion of the frontoturbinal region can be identified as an olfactory region. Although the *OMP* expression in R-001

(0.966) did not meet the criterion of 1.014, it was higher than expression levels observed in R-046, R-008, R-214, and R-215, which showed no *OMP* expression. Moreover, the expression of *ORs* in R-001 was distinctly higher than in R-046, R-008, R-214, and R-215, but lower than R-006 (Table 2). These findings led us to hypothesize that the sampled region R-001, specifically the posterior medial surface of ethmoturbinal II (Figure 1b), encompasses both respiratory and olfactory areas. It is commonly reported that respiratory and olfactory mucosae are distributed in a mosaic-like pattern, and this distribution may hold for cetaceans as well.

In this study, we conducted a microscopic examination of the ethmoturbinal II (H-001), the frontoturbinal (H-009), and the anterior region of the nasal chamber (H-046). These samples were assessed based on histological criteria proposed by Farnkopf et al. [29] and were likely identified as olfactory mucosa. However, it was the proximal region of the frontoturbinal (R-006) that suggested being the olfactory epithelium based on RNA-seq data (Table 3). Notably, the same region (H-009) exhibited a rich abundance of peripheral nerves, indicating its high sensitivity. On the other hand, within H-046, which was obtained from a more anterior region of the nasal cavity, dense clusters of vessels with thick walls were observed (Figure 5). This region may serve as a respiratory area where the vascular epithelium plays a role in thermoregulation.

Although the expressed *ORs* did not form a distinct cluster in the phylogenetic tree (Figure 4), it should be noted that the present study does not exclude the possibility of a concealed cluster containing *ORs* expressed in unexplored regions. One reason for this is that the distribution of olfactory receptor proteins, which mediate odoriferous stimuli to the olfactory bulb is not uniform across the olfactory epithelium [52–54]. Furthermore, the distribution pattern of the olfactory mucosa within the nasal chamber varies among lineages [55–58]. It is plausible that common minke whales possess additional *ORs* that contribute to their olfactory modality. Identifying such receptors would enhance our understanding of the molecular mechanisms underlying cetacean olfaction.

To comprehend the expression pattern of *ORs*, a thorough anatomical examination of the cetacean nasal chamber is indispensable. Our observations unveiled additional nasal turbinals positioned laterally to ethmoturbinals I and II (Figure 2b, FT and IT), which have been scarcely documented in cetaceans. However, due to the dearth of comprehensive anatomical data encompassing the entire nasal chamber, precise determination of the exact locations from which H-046 and R-046 were obtained remains elusive. Nasal turbinals can be broadly categorized into olfactory and respiratory turbinals, both of which play a pivotal role in unraveling mammalian aquatic adaptation [51,59,60]. In the nasal chamber of common minke whales, the anterior segment from which H-046 and R-046 were harvested is inferred to represent the respiratory region. It is conceivable that baleen whales also possess respiratory turbinals and investigating this structure is warranted in future studies. Although the present study primarily focused on the posterior region adjacent to the cribriform plate, gaining a comprehensive understanding of the entire labyrinthine architecture is crucial [61].

Fundamental anatomical data can function as an atlas during the dissection process. As highlighted by Farnkopf et al. [29], extracting the nasal chamber from the cranial bones of large whales presents a formidable challenge due to their remarkable dimensions, thickness, and robust structure. Identifying the nasal turbinals from sectional images can prove challenging, as their appearance exhibits variations with slight deviations in cutting angles. Moreover, the intricate nature of these structures impedes the efficient penetration of fixation solutions into the tissues. To surmount these sampling difficulties, a comprehensive description of the entire nasal chamber using CT imaging becomes imperative. Determining olfactory epithelium distribution emerges as the next crucial step. Predicting olfactory epithelium locations may be possible based on the surface coloration of the nasal mucosae. While the majority of the nasal mucosa in common minke whales displayed a pale pink hue, R-006, which exhibited distinct olfactory characteristics was obtained from an epithelium displaying a yellowish appearance. However, this coloration

may become indistinguishable once the sample is processed in formalin. A previous study tentatively proposed the limited usefulness of pigmentation in describing the distribution of olfactory epithelium in bowhead whales [29], indicating the need for further investigation.

The present study identified a pseudogene exclusively expressed in samples from external skin (Figure 4). This result is considered a form of biologically irregular expression, as the experiment was conducted successfully. The gene, identified as XM_028166200 in mBalAcu1.1 (GenBank accession GCF_949987535.1) is a pseudogene located outside OR clusters on the chromosome. Proper OR expression is governed by enhancer elements that target genes within a cluster; therefore, ORs outside the clusters are likely to fail in normal transcription [62]. The pseudo-OR expressed in skin samples is inferred to be one of these ORs and might be undergoing pseudogenization.

The entirety of the expressed ORs identified in this study exclusively belong to class-2 (Figure 4). Although there remains significant room for exploration, the probability of non-class-2 OR expression in common minke whales was presumed to be minimal even when thoroughly screening the entire lining mucosa of the nasal chamber. This presumption is rooted in observations during our dissection, which suggested the absence of the dorsal domain of the olfactory bulb in common minke whales. Non-class-2 olfactory receptors typically transmit input to the dorsal domain of the olfactory bulb. Consequently, we anticipated that non-class-2 ORs would not be expressed in the nasal mucosa of an animal lacking this specific region of the olfactory bulb. It has been documented that bowhead whales have also lost the dorsal domain of the olfactory bulb [27,28], and that common minke whales exhibit a dorsoventrally flattened olfactory bulb, akin to bowhead whales.

This study suggests that non-class-2 ORs do not partake in baleen whales' olfactory reception. In mice, non-class-2 ORs receive stimuli that trigger avoidance behaviors and project them into the dorsal domain of the olfactory bulb [63]. Hence, our findings imply the loss of the typical avoidance response to specific odorants, such as predators or putrefying substances, in whales.

Considering that sirenians, another lineage of fully aquatic mammals, still retain their olfactory organs and possess a large repertoire of ORs [30,33,64,65], the diminished olfactory ability of baleen whales cannot be solely attributed to their aquatic lifestyle, which restricts continuous respiration. One possible explanation for this lies in the necessity for discerning ingested foods. Anatomically, the esophagus of cetaceans is separated from the airway [66], preventing them from detecting smells emanating from the oral cavity. Genomic research has revealed a degeneration of taste, the other form of chemoreception, in cetaceans [32,67,68]. Furthermore, there is no anatomical description of taste buds in the tongues of baleen whales [69–72]. Consequently, baleen whales do not rely on chemosensory modalities to evaluate food in their mouths, which may contribute to their reduced olfactory capabilities.

Our genomic and histological investigations suggest that conserved class-2 ORs are responsible for olfaction in baleen whales. Specifically, the present study indicates that baleen whales can detect desirable odors, such as those associated with prey and potential mating partners. For instance, sporadically distributed dimethyl sulfide plays a crucial role in olfactory foraging for seabirds in marine environments [73–75]. A similar mechanism may operate in baleen whales [27,31]. This foraging strategy poses the risk of the inadvertent ingestion of marine plastic debris [76], underscoring the importance of assessing olfactory acuity in baleen whales. The present study establishes a foundational connection between rostral anatomy and genome. Subsequent inquiries hold promise for elucidating the natural, social, and behavioral biology of these creatures, contributing to their conservation efforts.

4. Materials and Methods

4.1. Sample Collection

The present study examined common minke whales obtained from the coastal regions of Japan. The specimens were acquired from seven animals (Table 1). In 2016, 16NPCK-

M009 and 16NPCK-M012 were procured during the second phase of the Japanese Whale Research Program under a special permit in the Western North Pacific (JARPNII). In 2018, 18NPCK-M001, 18NPCK-M006, and 18NPCK-M008 were obtained during the New Scientific Whale Research Program in the Western North Pacific (NEWREP-NP). In 2019, 19SK214 and 19SK215 were acquired during Japanese commercial whaling operations. The research programs adhered to the regulations outlined in Article VIII of the International Convention for the Regulation of Whaling (ICRW). All samples were collected in accordance with legal procedures.

The whales were harvested in the offshore waters of Hokkaido, Japan, and transported to fishing facilities for processing. To obtain the nasal mucosa, we meticulously dissected the occipital bones of common minke whales and extracted their brains to identify the entrances to the left and right olfactory tract tunnels. The head was then trimmed using a chain saw to create a bony block that encompassed the olfactory bulb tract and the nasal chamber. Upon observing the medial view of the sections (Figures 1a and 2a), we noted three prominent nasal turbinals, namely the lamina semicircularis and the ethmoturbinals I and II, arranged from the dorsal to ventral position [77], providing important indications for orientation.

The bony block, measuring 12 cm anteroposteriorly, 7 cm dorsoventrally, and 5 cm transversally was obtained from the left side of 16NPCK-M009. Subsequently, it was fixed in 10% formalin at the collection site and used for gross examination of the nasal chamber. A 5 mm square piece of mucosa was extracted from the posterior end of the frontoturbinal from the block, which was labeled H-009 for histological analysis.

We obtained two mucosal samples from 18NPCK-M001. Both samples were collected from the left side nasal mucosa of ethmoturbinal II, situated in front of the cribriform plate (Figure 1a,b). One sample was designated R-001 and frozen in RNA-later (Thermo Fisher Scientific Inc., Waltham, MA, USA) for subsequent RNA-seq analysis. The other sample, H-001 was fixed in 10% formalin for microscopic examination.

Another mucosal sample was acquired for RNA-seq analysis from 18NPCK-M006. The nasal chamber on the left side was carefully trimmed off the head (Figure 1c,d), promptly frozen, and transported to the laboratory. Subsequently, a 5 mm square mucosal sample was excised from the posterior end of the frontoturbinal region and designated R-006.

The bony block derived from specimen 18NPCK-M046 was sectioned in a transverse manner yielding two mucosal pieces extracted from the anterior portion of the right nasal chamber. The mucosal piece intended for RNA-seq analysis was labeled R-046, enclosed in a vinyl bag containing RNA-later, and stored in a freezer for preservation. Additionally, an adjacent mucosal piece, designated H-046 was collected and preserved in 10% formalin for subsequent microscopic examination.

To facilitate comparisons of gene expression across different organs, samples were also obtained from the olfactory bulb and external skin. We dissected 18NPCK-M008, excised the anterior 5 mm tip of the right olfactory bulb, and stored it in a freezer with RNA-later. This particular piece was labeled R-008. Furthermore, external skin samples were obtained from specimens 19SK214 and 19SK215, identified as R-214 and R-215, respectively, and preserved in a freezer.

The sampling procedures were recorded through both handwritten notes and digital macrophotography (Tough TG-5; Olympus Corporation, Tokyo, Japan). We quantified the postmortem interval as the duration between the animal's capture by boats above the sea and the preservation of the collected sample in either a freezer or formalin. The maximum recorded postmortem interval was 8.5 h (Table 1).

4.2. Gross Observation

The bony block obtained from 16NPCK-M009 was bisected along the medial wall to reveal the inner side of the nasal chamber. The cross-sections of the lamina semicircularis and ethmoturbinals I and II were observed, as shown in Figure 2. Upon removing the skeletal tissues of the medial nasal turbinals (ethmoturbinals I and II), the laterally positioned

turbinals became visible. The anatomical nomenclature used to identify the nasal turbinals was based on Ito et al. [78] and supplemented by relevant references [77,79].

4.3. RNA Expression

The RNA expression analysis in the present study employed the same methods described by Kishida et al. [44]. The OR genes were queried against the common minke whale genome assembly (GenBank accession GCA_000493695.1) [80] using the TBLASTN program in the BLAST+ v. 2.6.0 package [81] with a cut-off E-value of 1×10^{-5} . Deduced amino acid sequences of all intact ORs from green anole (*Anolis carolinensis*) and western clawed frog (*Xenopus tropicalis*), cow (*Bos taurus*), and mouse identified by Niimura [6] and Niimura et al. [82] were used as queries. Each obtained sequence was searched against the GenBank protein database using the BLASTX program [81]. If its best hit did not correspond to an OR, it was discarded. A sequence was deemed a non-functional pseudogene if it contained premature stop codons and/or frameshifts, or if it lacked five or more consecutive amino acids, including a transmembrane domain. Sequences interrupted by contig-gaps, though not classified as pseudogenes were labeled 'truncated'.

FATE (<https://github.com/Hikoyu/FATE>, accessed on 16 January 2023) was employed to search the common minke whale genome assembly (GenBank accession GCA_000493695.1) for OMP, using the annotated query sequence NW_006728793.1, identified as OMP, from GenBank Refseq GCF_000493695.1. The resulting single sequence found in GCA_000493695.1 was used for OMP mapping.

Total RNA was extracted from the nasal chamber mucosae (R-001, R-006, and R-046), olfactory bulb (R-008), and external skin (R-214, R-215) using the RNeasy Mini Kit (Qiagen, Hilden, Germany) following the manufacturer's guidelines. The olfactory bulb and external skin samples served as negative controls. The extracted RNA was used to construct paired-end sequencing libraries using the TruSeq Stranded mRNA LT Sample Prep Kit (Illumina Inc., San Diego, CA, USA). Subsequently, an Illumina NovaSeq platform (2×101 bp) was employed for sequencing, generating RNA-seq reads of the following sizes: R-001, 5.89 G bp; R-006, 4.57 G bp; R-046, 5.54 G bp; R-008, 5.37 G bp; R-214, 5.35 G bp; R-215, 6.03 G bp. Low-quality sequences and adapters were removed using Trimmomatic [83] v. 0.38 with the following parameters: ILLUMINACLIP: TruSeq3-PE-2.fa: 2:30:10, LEADING: 20, TRAILING: 20, SLIDINGWINDOW: 4:20, and MINLEN: 36. HISAT2 [84] v. 2.1.0 with default parameters was used to map trimmed RNA-seq reads to the conspecific genome assembly. Gene expression levels were quantified using fragments per kilobase of exon per million mapped fragments (FPKM) values with Cufflinks [85,86] v. 2.2.1 after removing duplicate reads. OR expression level was calculated by dividing it by β -actin gene and multiplying it by 100 to provide an expression percentage. Data analyses were performed using R (<https://www.R-project.org>, accessed on 28 July 2023) v. 4.2.2, with plots generated using the tidyverse package [87] v. 1.3.2 and ggplot2 [88] v. 3.4.0.

The annotated intact ORs of common minke whales were incorporated into a phylogenetic tree. The nucleotide sequences were aligned using MAFFT [89,90] v. 7. A suitable model was determined by ModelTest-NG [91,92] v. 0.1.7. Subsequently, a GTR + I + G4 model was selected, and the phylogenetic tree was constructed using RAxML-ng [93] v. 1.2.1 with the root set as non-class-2 ORs. The annotated intact ORs were numbered in descending order by FPKM values.

4.4. Histology Staining

The mucosal specimens underwent standard histological techniques. The samples were dehydrated using a series of ethanol concentrations and then cleared with xylene. Following infiltration and embedding in paraffin wax (melting point 56–58 °C), they were sectioned using a rotary microtome (PR-50; Yamato Kohki Industrial Co., Ltd., Saitama, Japan) into slices measuring 4–6 μ m. These sections were spread out on warm water, carefully transferred onto glass slides, and dried in an incubator at 60 °C for 30 min. During the staining process, they were immersed in deparaffinization solution, hydration medium,

and stain solution. Following mounting, the epithelial samples were examined and photographed using a digital microscope (VHX-7000; Keyence, Osaka, Japan; Axioscope 5 and AxioCam 503 color; Carl Zeiss, Jena, Germany). We evaluated whether these epithelial tissues qualified as olfactory epithelium based on criteria proposed by Farnkopf et al. [29]: epithelium constructed of basal cells, supporting cells, and olfactory sensory neurons; the presence of Bowman's glands; the absence of goblet cells, and the distance between the apical surface and nuclei of the supporting cells.

Supplementary Materials: The following supporting information can be downloaded at: <https://www.mdpi.com/article/10.3390/ijms25073855/s1>.

Author Contributions: Conceptualization, A.H. and T.K.; methodology, A.H., M.N. and T.K.; validation, M.N., H.K. and T.K.; formal analysis, A.H. and T.K.; investigation, A.H., G.N. and Y.F.; resources, Y.F. and H.K.; data curation, G.N., Y.F. and H.K.; writing—original draft preparation, A.H.; writing—review and editing, A.H., G.N., M.N. and T.K.; visualization, A.H.; funding acquisition, A.H. and H.K. All authors have read and agreed to the published version of the manuscript.

Funding: This study was financially supported by the Moritani Scholarship Foundation, Grant for Basic Science Research Projects from The Sumitomo Foundation (grant no. 180641), KAKENHI (Grant-in-Aid for JSPS fellows, grant no. 23KJ0956).

Institutional Review Board Statement: This study used post-mortem specimens and does not require Ethics Committee or Institutional Review Board approval. The specimens were obtained legally and ethically from Japanese research and commercial whaling activities with the permission of the Government of Japan.

Data Availability Statement: All sequence reads were deposited in the DDBJ Sequence Read Archive under BioProject accession no. PRJDB16252.

Acknowledgments: We are grateful to the late Hideyoshi Yoshida for helping a lot during sample collection. We thank Saeko Kumagai and Hiroto Murase for collecting the skin samples; Kai Ito for identifying nasal turbinates; Masahide Hasobe for staining; Takashi Sakamoto for preparing surgical instruments; Andrew Shedlock for improving the manuscript; and our Lab members. Computations were partially performed on the NIG supercomputer at ROIS National Institute of Genetics.

Conflicts of Interest: The authors declare no conflicts of interest. The funders had no role in the design of the study; in the collection, analyses, or interpretation of data; in the writing of the manuscript; or in the decision to publish the results.

References

1. Doty, R.L. Odor-guided behavior in mammals. *Experientia* **1986**, *42*, 257–271. [[CrossRef](#)] [[PubMed](#)]
2. Nei, M.; Niimura, Y.; Nozawa, M. The evolution of animal chemosensory receptor gene repertoires: Roles of chance and necessity. *Nat. Rev. Genet.* **2008**, *9*, 951–963. [[CrossRef](#)]
3. Corona, R.; Lévy, F. Chemical olfactory signals and parenthood in mammals. *Horm. Behav.* **2015**, *68*, 77–90. [[CrossRef](#)] [[PubMed](#)]
4. Buck, L.; Axel, R. A novel multigene family may encode odorant receptors: A molecular basis for odor recognition. *Cell* **1991**, *65*, 175–187. [[CrossRef](#)] [[PubMed](#)]
5. Niimura, Y.; Nei, M. Evolutionary dynamics of olfactory receptor genes in fishes and tetrapods. *Proc. Natl. Acad. Sci. USA* **2005**, *102*, 6039–6044. [[CrossRef](#)] [[PubMed](#)]
6. Niimura, Y. On the origin and evolution of vertebrate olfactory receptor genes: Comparative genome analysis among 23 chordate species. *Genome Biol. Evol.* **2009**, *1*, 34–44. [[CrossRef](#)] [[PubMed](#)]
7. Malnic, B.; Hirono, J.; Sato, T.; Buck, L.B. Combinatorial receptor codes for odors. *Cell* **1999**, *96*, 713–723. [[CrossRef](#)] [[PubMed](#)]
8. Saito, H.; Chi, Q.; Zhuang, H.; Matsunami, H.; Mainland, J.D. Odor coding by a Mammalian receptor repertoire. *Sci. Signal.* **2009**, *2*, ra9. [[CrossRef](#)]
9. Pihlström, H.; Fortelius, M.; Hemilä, S.; Forsman, R.; Reuter, T. Scaling of mammalian ethmoid bones can predict olfactory organ size and performance. *Proc. R. Soc. B Biol. Sci.* **2005**, *272*, 957–962. [[CrossRef](#)] [[PubMed](#)]
10. Niimura, Y. Evolutionary dynamics of olfactory receptor genes in chordates: Interaction between environments and genomic contents. *Hum. Genom.* **2009**, *4*, 107. [[CrossRef](#)]
11. Zhou, Y.; Shearwin-Whyatt, L.; Li, J.; Song, Z.; Hayakawa, T.; Stevens, D.; Felon, J.C.; Peel, E.; Cheng, Y.; Pajpach, F.; et al. Platypus and echidna genomes reveal mammalian biology and evolution. *Nature* **2021**, *592*, 756–762. [[CrossRef](#)]
12. Moran, D.T.; Rowley, J.C.; Jafek, B.W.; Lovell, M.A. The fine structure of the olfactory mucosa in man. *J. Neurocytol.* **1982**, *11*, 721–746. [[CrossRef](#)] [[PubMed](#)]

13. Bird, D.J.; Murphy, W.J.; Fox-Rosales, L.; Hamid, I.; Eagle, R.A.; Van Valkenburgh, B. Olfaction written in bone: Cribriform plate size parallels olfactory receptor gene repertoires in Mammalia. *Proc. R. Soc. B Biol. Sci.* **2018**, *285*, 20180100. [[CrossRef](#)] [[PubMed](#)]
14. Niimura, Y.; Nei, M. Evolution of olfactory receptor genes in the human genome. *Proc. Natl. Acad. Sci. USA* **2003**, *100*, 12235–12240. [[CrossRef](#)] [[PubMed](#)]
15. Niimura, Y.; Nei, M. Extensive gains and losses of olfactory receptor genes in mammalian evolution. *PLoS ONE* **2007**, *2*, e708. [[CrossRef](#)] [[PubMed](#)]
16. Roe, L.J.; Thewissen, J.G.M.; Quade, J.; O'Neil, J.R.; Bajpai, S.; Sahni, A.; Hussain, S.T. Isotopic Approaches to Understanding the Terrestrial-to-Marine Transition of the Earliest Cetaceans. In *The Emergence of Whales: Evolutionary Patterns in the Origin of Cetacea*; Thewissen, J.G.M., Ed.; Springer: Boston, MA, USA, 1998; pp. 399–422. [[CrossRef](#)]
17. Clementz, M.T.; Goswami, A.; Gingerich, P.D.; Koch, P.L. Isotopic records from early whales and sea cows: Contrasting patterns of ecological transition. *J. Vertebr. Paleontol.* **2006**, *26*, 355–370. [[CrossRef](#)]
18. Gatesy, J.; Geisler, J.H.; Chang, J.; Buell, C.; Berta, A.; Meredith, R.W.; Springer, M.S.; McGowen, M.R. A phylogenetic blueprint for a modern whale. *Mol. Phylogenet. Evol.* **2013**, *66*, 479–506. [[CrossRef](#)] [[PubMed](#)]
19. Nikaido, M.; Rooney, A.P.; Okada, N. Phylogenetic relationships among cetartiodactyls based on insertions of short and long interspersed elements: Hippopotamuses are the closest extant relatives of whales. *Proc. Natl. Acad. Sci. USA* **1999**, *96*, 10261–10266. [[CrossRef](#)] [[PubMed](#)]
20. Nikaido, M.; Matsuno, F.; Abe, H.; Shimamura, M.; Hamilton, H.; Matsubayashi, H.; Okada, N. Evolution of CHR-2 SINEs in cetartiodactyl genomes: Possible evidence for the monophyletic origin of toothed whales. *Mamm. Genome* **2001**, *12*, 909–915. [[CrossRef](#)]
21. Miller, P.J.O.; Roos, M.M.H. Breathing. In *Encyclopedia of Marine Mammals*; Würsig, B., Thewissen, J.G.M., Kovacs, K.M., Eds.; Academic Press: San Diego, CA, USA, 2018; pp. 140–143. [[CrossRef](#)]
22. Chu, K.C. Dive times and ventilation patterns of singing humpback whales (*Megaptera novaeangliae*). *Can. J. Zool.* **1988**, *66*, 1322–1327. [[CrossRef](#)]
23. Hedley, S.L.; Bannister, J.L.; Dunlop, R.A. Abundance estimates of Southern Hemisphere Breeding Stock 'D' humpback whales from aerial and land-based surveys off Shark Bay, Western Australia, 2008. *J. Cetacean Res. Manag.* **2011**, *3*, 209–221. [[CrossRef](#)]
24. Godfrey, S.J.; Geisler, J.; Fitzgerald, E.M.G. On the olfactory anatomy in an archaic whale (Protocetidae, Cetacea) and the minke whale *Balaenoptera acutorostrata* (Balaenopteridae, Cetacea). *Anat. Rec.* **2013**, *296*, 257–272. [[CrossRef](#)]
25. Ichishima, H. The ethmoid and presphenoid of cetaceans. *J. Morphol.* **2016**, *277*, 1661–1674. [[CrossRef](#)] [[PubMed](#)]
26. Hirose, A.; Kishida, T.; Nakamura, G. Nasal mucosa resembling an olfactory system in the common minke whale (*Balaenoptera acutorostrata*). *Cetacean Popul. Stud.* **2018**, *1*, 25–28. [[CrossRef](#)]
27. Thewissen, J.G.M.; George, J.; Rosa, C.; Kishida, T. Olfaction and brain size in the bowhead whale (*Balaena mysticetus*). *Mar. Mammal Sci.* **2011**, *27*, 282–294. [[CrossRef](#)]
28. Kishida, T.; Thewissen, J.; Usip, S.; Suydam, R.S.; George, J.C. Organization and distribution of glomeruli in the bowhead whale olfactory bulb. *PeerJ* **2015**, *3*, e897. [[CrossRef](#)] [[PubMed](#)]
29. Farnkopf, I.C.; George, J.C.; Kishida, T.; Hillmann, D.J.; Suydam, R.S.; Thewissen, J.G.M. Olfactory epithelium and ontogeny of the nasal chambers in the bowhead whale (*Balaena mysticetus*). *Anat. Rec.* **2022**, *305*, 643–667. [[CrossRef](#)] [[PubMed](#)]
30. Han, W.; Wu, Y.; Zeng, L.; Zhao, S. Building the Chordata Olfactory Receptor Database using more than 400,000 receptors annotated by Genome2OR. *Sci. China Life Sci.* **2022**, *65*, 2539–2551. [[CrossRef](#)] [[PubMed](#)]
31. Kishida, T. Olfaction of aquatic amniotes. *Cell Tissue Res.* **2021**, *383*, 353–365. [[CrossRef](#)]
32. Kishida, T.; Thewissen, J.; Hayakawa, T.; Imai, H.; Agata, K. Aquatic adaptation and the evolution of smell and taste in whales. *Zool. Lett.* **2015**, *1*, 9. [[CrossRef](#)]
33. Christmas, M.J.; Kaplow, I.M.; Genereux, D.P.; Dong, M.X.; Hughes, G.M.; Li, X.; Sullivan, P.F.; Hindle, A.G.; Andrews, G.; Armstrong, J.C.; et al. Evolutionary constraint and innovation across hundreds of placental mammals. *Science* **2023**, *380*, eabn3943. [[CrossRef](#)]
34. Danciger, E.; Mettling, C.; Vidal, M.; Morris, R.; Margolis, F. Olfactory marker protein gene: Its structure and olfactory neuron-specific expression in transgenic mice. *Proc. Natl. Acad. Sci. USA* **1989**, *86*, 8565–8569. [[CrossRef](#)] [[PubMed](#)]
35. Buiakova, O.I.; Baker, H.; Scott, J.W.; Farbman, A.; Kream, R.; Grillo, M.; Franzen, L.; Richman, M.; Davis, L.M.; Abbondanzo, S.; et al. Olfactory marker protein (OMP) gene deletion causes altered physiological activity of olfactory sensory neurons. *Proc. Natl. Acad. Sci. USA* **1996**, *93*, 9858–9863. [[CrossRef](#)] [[PubMed](#)]
36. Kishida, T.; Thewissen, J.G.M. Evolutionary changes of the importance of olfaction in cetaceans based on the olfactory marker protein gene. *Gene* **2012**, *492*, 349–353. [[CrossRef](#)] [[PubMed](#)]
37. Springer, M.; Gatesy, J. Inactivation of the olfactory marker protein (OMP) gene in river dolphins and other odontocete cetaceans. *Mol. Phylogenet. Evol.* **2017**, *109*, 375–387. [[CrossRef](#)] [[PubMed](#)]
38. Cranford, T.W.; Amundin, M.; Norris, K.S. Functional morphology and homology in the odontocete nasal complex: Implications for sound generation. *J. Morphol.* **1996**, *228*, 223–285. [[CrossRef](#)]
39. Berta, A.; Ekdale, E.G.; Cranford, T.W. Review of the cetacean nose: Form, function, and evolution. *Anat. Rec.* **2014**, *297*, 2205–2215. [[CrossRef](#)] [[PubMed](#)]
40. Hirose, A.; Kodera, R.; Uekusa, Y.; Katsumata, H.; Katsumata, E.; Nakamura, G.; Kato, H. Comparative anatomy of and around the posterior nasofrontal sac of a beluga whale. *Mar. Mammal Sci.* **2022**, *38*, 1272–1285. [[CrossRef](#)]

41. Bouchard, B.; Barnagaud, J.-Y.; Poupard, M.; Glotin, H.; Gauffier, P.; Ortiz, S.T.; Lisney, T.J.; Campagna, S.; Rasmussen, M.; Célérier, A. Behavioural responses of humpback whales to food-related chemical stimuli. *PLoS ONE* **2019**, *14*, e0212515. [[CrossRef](#)]
42. Bouchard, B.; Barnagaud, J.; Verborgh, P.; Gauffier, P.; Campagna, S.; Célérier, A. A field study of chemical senses in bottlenose dolphins and pilot whales. *Anat. Rec.* **2022**, *305*, 668–679. [[CrossRef](#)]
43. Go, Y.; Niimura, Y. Similar numbers but different repertoires of olfactory receptor genes in humans and chimpanzees. *Mol. Biol. Evol.* **2008**, *25*, 1897–1907. [[CrossRef](#)] [[PubMed](#)]
44. Kishida, T.; Go, Y.; Tatsumoto, S.; Tatsumi, K.; Kuraku, S.; Toda, M. Loss of olfaction in sea snakes provides new perspectives on the aquatic adaptation of amniotes. *Proc. R. Soc. B* **2019**, *286*, 20191828. [[CrossRef](#)] [[PubMed](#)]
45. Chen, Z.; Zhao, H.; Fu, N.; Chen, L. The diversified function and potential therapy of ectopic olfactory receptors in non-olfactory tissues. *J. Cell. Physiol.* **2018**, *233*, 2104–2115. [[CrossRef](#)] [[PubMed](#)]
46. Parmentier, M.; Libert, F.; Schurmans, S.; Schiffmann, S.; Lefort, A.; Eggerickx, D.; Ledent, C.; Mollereau, C.; Gérard, C.; Perret, J.; et al. Expression of members of the putative olfactory receptor gene family in mammalian germ cells. *Nature* **1992**, *355*, 453–455. [[CrossRef](#)] [[PubMed](#)]
47. Spehr, M.; Gisselmann, G.; Poplawski, A.; Riffell, J.A.; Wetzel, C.H.; Zimmer, R.K.; Hatt, H. Identification of a testicular odorant receptor mediating human sperm chemotaxis. *Science* **2003**, *299*, 2054–2058. [[CrossRef](#)] [[PubMed](#)]
48. Fukuda, N.; Yomogida, K.; Okabe, M.; Touhara, K. Functional characterization of a mouse testicular olfactory receptor and its role in chemosensing and in regulation of sperm motility. *J. Cell Sci.* **2004**, *117*, 5835–5845. [[CrossRef](#)] [[PubMed](#)]
49. Rouquier, S.; Giorgi, D. Olfactory receptor gene repertoires in mammals. *Mutat. Res./Fundam. Mol. Mech. Mutagen.* **2007**, *616*, 95–102. [[CrossRef](#)] [[PubMed](#)]
50. Neuhaus, E.M.; Zhang, W.; Gelis, L.; Deng, Y.; Noldus, J.; Hatt, H. Activation of an olfactory receptor inhibits proliferation of prostate cancer cells. *J. Biol. Chem.* **2009**, *284*, 16218–16225. [[CrossRef](#)] [[PubMed](#)]
51. Van Valkenburgh, B.; Pang, B.; Bird, D.; Curtis, A.; Yee, K.; Wysocki, C.; Craven, B.A. Respiratory and olfactory turbinals in feliform and caniniform carnivorans: The influence of snout length. *Anat. Rec.* **2014**, *297*, 2065–2079. [[CrossRef](#)]
52. Ressler, K.J.; Sullivan, S.L.; Buck, L.B. A zonal organization of odorant receptor gene expression in the olfactory epithelium. *Cell* **1993**, *73*, 597–609. [[CrossRef](#)]
53. Vassar, R.; Ngai, J.; Axel, R. Spatial segregation of odorant receptor expression in the mammalian olfactory epithelium. *Cell* **1993**, *74*, 309–318. [[CrossRef](#)] [[PubMed](#)]
54. Marchand, J.E.; Yang, X.; Chikaraishi, D.; Krieger, J.; Breer, H.; Kauer, J.S. Olfactory receptor gene expression in tiger salamander olfactory epithelium. *J. Comp. Neurol.* **2004**, *474*, 453–467. [[CrossRef](#)] [[PubMed](#)]
55. Smith, T.D.; Eiting, T.P.; Bhatnagar, K.P. A Quantitative study of olfactory, non-olfactory, and vomeronasal epithelia in the nasal fossa of the bat *Megaderma lyra*. *J. Mamm. Evol.* **2012**, *19*, 27–41. [[CrossRef](#)]
56. Ruf, I. Comparative anatomy and systematic implications of the turbinal skeleton in Lagomorpha (Mammalia). *Anat. Rec.* **2014**, *297*, 2031–2046. [[CrossRef](#)] [[PubMed](#)]
57. Smith, T.D.; Eiting, T.P.; Bonar, C.J.; Craven, B.A. Nasal morphometry in marmosets: Loss and redistribution of olfactory surface area. *Anat. Rec.* **2014**, *297*, 2093–2104. [[CrossRef](#)] [[PubMed](#)]
58. Ito, K.; Tu, V.T.; Eiting, T.P.; Nojiri, T.; Koyabu, D. On the embryonic development of the nasal turbinals and their homology in bats. *Front. Cell Dev. Biol.* **2021**, *9*, 613545. [[CrossRef](#)] [[PubMed](#)]
59. Van Valkenburgh, B.; Curtis, A.; Samuels, J.X.; Bird, D.; Fulkerson, B.; Meachen-Samuels, J.; Slater, G.J. Aquatic adaptations in the nose of carnivorans: Evidence from the turbinates. *J. Anat.* **2011**, *218*, 298–310. [[CrossRef](#)]
60. Martinez, Q.; Clavel, J.; Esselstyn, J.A.; Achmadi, A.S.; Grohé, C.; Piro, N.; Fabre, P.-H. Convergent evolution of olfactory and thermoregulatory capacities in small amphibious mammals. *Proc. Natl. Acad. Sci. USA* **2020**, *117*, 8958–8965. [[CrossRef](#)] [[PubMed](#)]
61. Van Valkenburgh, B.; Smith, T.D.; Craven, B.A. Tour of a labyrinth: Exploring the vertebrate nose. *Anat. Rec.* **2014**, *297*, 1975–1984. [[CrossRef](#)] [[PubMed](#)]
62. Iwata, T.; Niimura, Y.; Kobayashi, C.; Shirakawa, D.; Suzuki, H.; Enomoto, T.; Touhara, K.; Yoshihara, Y.; Hirota, J. A long-range cis-regulatory element for class I odorant receptor genes. *Nat. Commun.* **2017**, *8*, 885. [[CrossRef](#)]
63. Kobayakawa, K.; Kobayakawa, R.; Matsumoto, H.; Oka, Y.; Imai, T.; Ikawa, M.; Okabe, M.; Ikeda, T.; Itohara, S.; Kikusui, T.; et al. Innate versus learned odour processing in the mouse olfactory bulb. *Nature* **2007**, *450*, 503–508. [[CrossRef](#)] [[PubMed](#)]
64. Barboza, M.L.B.; Larkin, I.V. Gross and microscopic anatomy of the nasal cavity, including olfactory epithelium, of the Florida manatee (*Trichechus manatus latirostris*). *Aquat. Mamm.* **2020**, *46*, 274–284. [[CrossRef](#)]
65. Policarpo, M.; Baldwin, M.W.; Casane, D.; Salzburger, W. Diversity and evolution of the vertebrate chemoreceptor gene repertoire. *Nat. Commun.* **2024**, *15*, 1421. [[CrossRef](#)]
66. Tyack, P.L.; Miller, E.H. Vocal anatomy, acoustic communication and echolocation. In *Marine Mammal Biology: An Evolutionary Approach*; Blackwell Science: Hoboken, NJ, USA, 2002; pp. 142–184.
67. Feng, P.; Zheng, J.; Rossiter, S.J.; Wang, D.; Zhao, H. Massive Losses of Taste Receptor Genes in Toothed and Baleen Whales. *Genome Biol. Evol.* **2014**, *6*, 1254–1265. [[CrossRef](#)] [[PubMed](#)]
68. Zhu, K.; Zhou, X.; Xu, S.; Sun, D.; Ren, W.; Zhou, K.; Yang, G. The loss of taste genes in cetaceans. *BMC Evol. Biol.* **2014**, *14*, 218. [[CrossRef](#)] [[PubMed](#)]
69. Sonntag, C.F. The Comparative Anatomy of the Tongues of the Mammalia.—VII. Cetacea, Sirenia, and Ungulata. *Proc. Zool. Soc. Lond.* **1922**, *92*, 639–657. [[CrossRef](#)]

70. Ogawa, T.; Shida, T. On the sensory tubercles of lips and oral cavity in the sei and fin whale. *Sci. Rep. Whales Res. Inst.* **1950**, *3*, 1–16.
71. Tarpley, R.J. Gross and Microscopic Anatomy of the Tongue and Gastrointestinal Tract of the Bowhead Whale (*Balaena mysticetus*). Ph.D. Thesis, Texas A&M University, College Station, TX, USA, December 1985.
72. Schulte, H.v.W. Anatomy of a foetus of *Balaenoptara borealis*. *Monogr. Pac. Cetacea* **1916**, *1*, 389–502.
73. Nevitt, G.A. Olfactory foraging by Antarctic procellariiform seabirds: Life at high Reynolds numbers. *Biol. Bull.* **2000**, *198*, 245–253. [[CrossRef](#)]
74. Dell’Ariccia, G.; Celerier, A.; Gabriot, M.; Palmas, P.; Massa, B.; Bonadonna, F. Olfactory foraging in temperate waters: Sensitivity to dimethylsulphide of shearwaters in the Atlantic Ocean and Mediterranean Sea. *J. Exp. Biol.* **2014**, *217*, 1701–1709. [[CrossRef](#)]
75. Owen, K.; Saeki, K.; Warren, J.D.; Bocconcelli, A.; Wiley, D.N.; Ohira, S.-I.; Bombosch, A.; Toda, K.; Zitterbart, D.P. Natural dimethyl sulfide gradients would lead marine predators to higher prey biomass. *Commun. Biol.* **2021**, *4*, 149. [[CrossRef](#)]
76. Savoca, M.S.; Wohlfeil, M.E.; Ebeler, S.E.; Nevitt, G.A. Marine plastic debris emits a keystone infochemical for olfactory foraging seabirds. *Sci. Adv.* **2016**, *2*, e1600395. [[CrossRef](#)]
77. Klima, M. *Development of the Cetacean Nasal Skull*; Springer: Berlin/Heidelberg, Germany, 1999. [[CrossRef](#)]
78. Ito, K.; Kodeara, R.; Koyasu, K.; Martinez, Q.; Koyabu, D. The development of nasal turbinal morphology of moles and shrews. *Vertebr. Zool.* **2022**, *72*, 857–881. [[CrossRef](#)]
79. Maier, W.; Ruf, I. Morphology of the nasal capsule of primates—With special reference to *Daubentonia* and *Homo*. *Anat. Rec.* **2014**, *297*, 1985–2006. [[CrossRef](#)] [[PubMed](#)]
80. Yim, H.-S.; Cho, Y.S.; Guang, X.; Kang, S.G.; Jeong, J.-Y.; Cha, S.-S.; Oh, H.-M.; Lee, J.-H.; Yang, E.C.; Kwon, K.K.; et al. Minke whale genome and aquatic adaptation in cetaceans. *Nat. Genet.* **2014**, *46*, 88–92. [[CrossRef](#)]
81. Camacho, C.; Coulouris, G.; Avagyan, V.; Ma, N.; Papadopoulos, J.; Bealer, K.; Madden, T.L. BLAST+: Architecture and applications. *BMC Bioinform.* **2009**, *10*, 421. [[CrossRef](#)]
82. Niimura, Y.; Matsui, A.; Touhara, K. Extreme expansion of the olfactory receptor gene repertoire in African elephants and evolutionary dynamics of orthologous gene groups in 13 placental mammals. *Genome Res.* **2014**, *24*, 1485–1496. [[CrossRef](#)] [[PubMed](#)]
83. Bolger, A.M.; Lohse, M.; Usadel, B. Trimmomatic: A flexible trimmer for Illumina sequence data. *Bioinformatics* **2014**, *30*, 2114–2120. [[CrossRef](#)] [[PubMed](#)]
84. Kim, D.; Langmead, B.; Salzberg, S.L. HISAT: A fast spliced aligner with low memory requirements. *Nat. Methods* **2015**, *12*, 357–360. [[CrossRef](#)]
85. Trapnell, C.; Williams, B.A.; Pertea, G.; Mortazavi, A.; Kwan, G.; Van Baren, M.J.; Salzberg, S.L.; Wold, B.J.; Pachter, L. Transcript assembly and quantification by RNA-Seq reveals unannotated transcripts and isoform switching during cell differentiation. *Nat. Biotechnol.* **2010**, *28*, 511–515. [[CrossRef](#)]
86. Roberts, A.; Trapnell, C.; Donaghey, J.; Rinn, J.L.; Pachter, L. Improving RNA-Seq expression estimates by correcting for fragment bias. *Genome Biol.* **2011**, *12*, R22. [[CrossRef](#)] [[PubMed](#)]
87. Wickham, H.; Averick, M.; Bryan, J.; Chang, W.; McGowan, L.D.; François, R.; Golemund, G.; Hayes, A.; Henry, L.; Hester, J.; et al. Welcome to the tidyverse. *J. Open Source Softw.* **2019**, *4*, 1686. [[CrossRef](#)]
88. Wickham, H. *ggplot2: Elegant Graphics for Data Analysis*; Springer: New York, NY, USA, 2016; 182p.
89. Kuraku, S.; Zmasek, C.M.; Nishimura, O.; Katoh, K. aLeaves facilitates on-demand exploration of metazoan gene family trees on MAFFT sequence alignment server with enhanced interactivity. *Nucleic Acids Res.* **2013**, *41*, W22–W28. [[CrossRef](#)]
90. Katoh, K.; Rozewicki, J.; Yamada, K.D. MAFFT online service: Multiple sequence alignment, interactive sequence choice and visualization. *Brief. Bioinform.* **2019**, *20*, 1160–1166. [[CrossRef](#)] [[PubMed](#)]
91. Darriba, D.; Posada, D.; Kozlov, A.M.; Stamatakis, A.; Morel, B.; Flouri, T. ModelTest-NG: A new and scalable tool for the selection of DNA and protein evolutionary models. *Mol. Biol. Evol.* **2019**, *37*, 291–294. [[CrossRef](#)] [[PubMed](#)]
92. Flouri, T.; Izquierdo-Carrasco, F.; Darriba, D.; Aberer, A.; Nguyen, L.-T.; Minh, B.; Von Haeseler, A.; Stamatakis, A. The Phylogenetic Likelihood Library. *Syst. Biol.* **2014**, *64*, 356–362. [[CrossRef](#)]
93. Kozlov, A.M.; Darriba, D.; Flouri, T.; Morel, B.; Stamatakis, A. RAXML-NG: A fast, scalable and user-friendly tool for maximum likelihood phylogenetic inference. *Bioinformatics* **2019**, *35*, 4453–4455. [[CrossRef](#)]

Disclaimer/Publisher’s Note: The statements, opinions and data contained in all publications are solely those of the individual author(s) and contributor(s) and not of MDPI and/or the editor(s). MDPI and/or the editor(s) disclaim responsibility for any injury to people or property resulting from any ideas, methods, instructions or products referred to in the content.